Rose-Hulman Undergraduate Mathematics Journal

Volume 4
Issue 2

Article 6

Long Term Dynamics for Two Three-Species Food Webs

Brian Bockelman
University of Nebraska-Lincoln

Elizabeth Green
University of Nebraska-Lincoln, egreen@math.unl.edu

Leslie Lippitt
Iowa State University

Jason Sherman
Kent State University, jsherman@kent.edu

Long Term Dynamics for Two Three-Species Food Webs*

B. Bockelman, E. Green, L. Lippitt, J. Sherman

October 28, 2003

Abstract

In this paper, we analyze two possible scenarios for food webs with two prey and one predator (a food web is similar to a food chain except that in a web we have more than one species at some levels). In neither scenario do the prey compete, rather the scenarios differ in the selection method used by the predator. We determine how the dynamics depend on various parameter values. For some parameter values, one or more species dies out. For other parameter values, all species co-exist at equilibrium. For still other parameter values, the populations behave cyclically. We have even discovered parameter values for which the system exhibits chaos and has a positive Lyapunov exponent. Our analysis relies on common techniques such as nullcline analysis, equilibrium analysis and singular perturbation analysis.

1 Introduction

In this paper we analyze two possible scenarios for food webs with two prey and one predator. In neither scenario do the prey compete, rather the scenarios differ in the selection method used by the predator. In the first model, both prey are available to the predator at all times and the predator does not distinguish between the two, however one is easier to catch. In the second scenario, only one prey is available at a time.

Through our analysis, we will determine how the dynamics of the population depend on the parameter values. For some parameter values, one or more species dies out. For

*This work was done as a part of the Nebraska REU in Applied Math Program supported by the National Science Foundation, grant #0139499. Faculty advisors were Bo Deng and Gwendolen Hines

other parameter values, all species co-exist at equilibrium. For still other parameter values, the populations behave cyclically. Many different cycles are possible. We have even discovered parameter values for which the system exhibits chaos and has a positive Lyapunov exponent. Perhaps surprisingly, such complicated behavior only exists in the disjointly-available prey case.

The type of analysis that we use is a mixture of nullcline analysis, singular perturbation analysis and numerical experimentation. These methods will be explained in the body of the paper. In the remainder of the introduction, we provide some background on predator-prey models. These ideas will be used in the sections below to construct our models.

For our models, we will assume that the prey grows logistically in the absence of predators. If $X(t)$ is the number of prey, and there are no predators, then the logistic model gives us

$$\frac{dX}{dt} = rX(1 - X/K)$$

where r is the birth rate and K is the carrying capacity (the maximum population that the environment can theoretically sustain). We will assume that the predator dies off exponentially in the absence of prey; that is if $Y(t)$ is the number of predators then

$$\frac{dY}{dt} = -dY$$

where d is the death rate. We must also include in our model terms for the effects of predation. By what amount does predation decrease the growth rate of the prey and increase the growth rate of the predator? In his seminal paper, C. S. Holling ([1]), in 1959, devised an experiment from which he obtained what is now known as the Holling type-II predation model. In this famous experiment, the 'prey' were sandpaper discs thumb-tacked to a three-foot square table. The 'predator' was a blindfolded person who was instructed to locate prey by tapping on the table with her finger. As each disc was found, it was removed and set to one side before searching continued. The experiment was repeated several times, with different disc densities. A graph of Number of Discs Picked Up vs Number of Discs per 9 Square Feet is shown in Figure 1.1. As can be seen, the Number of Discs Picked Up levels off when the density of discs becomes large. This is because when large numbers of discs are available, a larger proportion of time must be spent in removing discs, rather than searching. The process of removing discs is called *prey handling*. If n is the number of discs found then

$$n = aT_s x \tag{1.1}$$

where x is the total number of discs, T_s is the amount of time available for searching, and a is a constant equal to the rate of searching multiplied by the probability of finding a disc. This constant will be termed the *instantaneous rate of discovery*. If a fixed amount of time, T_t, is allowed for the experiment, then the total search time available is

$$T_s = T_t - bn \tag{1.2}$$

where b is the amount of time it takes to handle one disc (the *prey handling time*). If we substitute T_s in 1.1 by the expression in 1.2 and solve for n, we obtain

$$\frac{n}{T_t} = \frac{ax}{1+abx} = \frac{\frac{1}{b}x}{\frac{1}{ab}+x} = \frac{px}{H+x}$$

where $p = 1/b$ and $H = 1/ab$. The term $\frac{n}{T_t}$ is the number of prey caught by the predator per unit of time. Notice that $\lim_{n\to\infty} \frac{n}{T_t} = p$ and so p is the *maximum capture rate*, and that when $x = H$, the number of discs found is half the maximum. H is commonly referred to as the *half saturation constant*. The constants a and b can be computed from the data. If we graph this function, we see it has the same shape as the graph in Figure 1.1.

In real populations, Holling conjectured, predation is similar to disc-searching and the predation term should have the form $px/(H+x)$. Researchers have found this to be an accurate model for many predator-prey situations and it is commonly used today (see [2] and [3]). In the next Sections, we will put growth and predation terms together to build suitable food web models and we will use the techniques mentioned above to analyze them.

2 Analysis of the 1-Predator 1-Prey Model

We begin by analyzing the model with only one predator and one prey. This gives us an opportunity to illustrate the methods in a simpler context.

2.1 The Model

Let X be the prey and Y be the predator. If we assume the prey grow logistically in the absence of predators and the predators die off exponentially in the absence of prey, and if we use a Holling type-II predation term so that the number of prey captured per predator per time is $pX/(H+X)$, we get the model

$$\begin{aligned} \tfrac{dX}{dt} &= rX(1-X/K) - \tfrac{pX}{H+X}Y \\ \tfrac{dY}{dt} &= \tfrac{bpX}{H+X}Y - dY \end{aligned}$$

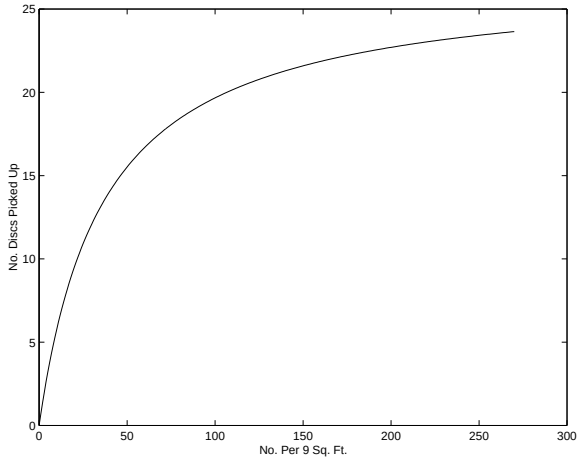

Figure 1.1: Number of Discs Picked Up vs Number of Discs per 9 Square Feet

The parameter b here is called the *birth-to-consumption ratio* and measures the positive effect that capturing a prey has on a predator's ability to reproduce.

We want to rescale this model in order to both simplify it and nondimensionalize it. For our dimensionless variables, we choose $x = X/K$ and $y = Y/K_y$ where $K_y = rK/p$. The reason for our choice of X is clear. The new variable x is dimensionless and gives the population as a fraction of the carrying capacity. We want to define y similarly. It seems reasonable from a biological point of view to expect that the carrying capacity for Y, that is K_y, will be approximately the population at which the maximum predator capture rate, pK_y, is equal to the maximum growth rate of the prey, rK. This gives $K_y = rK/p$, which gives us a convenient re-scaling for y.

We also rescale time so that we use the time-scale determined by the predator's reproduction rate; thus $\bar{t} = bpt$. We define other simplifying parameters: $\beta = H/K$ measures predator efficiency, $\delta = d/bp$ measures the ratio of the predator's death rate to the predator's birth rate, and $\zeta = bp/r$ measures the ratio of birth rates. With these new variables and parameters, we get the system

$$\begin{array}{rcl} \zeta\dfrac{dx}{dt} & = & x\left(1 - x - \frac{y}{\beta+x}\right) := xf(x,y) \\ \dfrac{dy}{dt} & = & y\left(\frac{x}{\beta+x} - \delta\right) := yg(x) \end{array} \tag{2.1}$$

In nature it is often the case that the predator birth rate is much slower than that of the prey. One might imagine cattle and grass, for example, or humans and rabbits. In this

case ζ is very small and so, since $\dot{x} = \frac{1}{\zeta} x f(x, y)$, x changes very rapidly compared to y, provided f is not near zero. In this case, we say that the system is *singularly perturbed* and we can take advantage of the two time scales to easily construct an approximate orbit, called the *singular orbit*. We do this in Section II.3. It is also important to identify and analyze the equilibria which we do in the next section.

2.2 Nullclines and Equilibria

We begin by determining the nullclines (places where one or the other of the derivatives is zero) of the system (1). The x-nullclines (where $\frac{dx}{dt} = 0$) are the axis $x = 0$ and the parabola $y = (1 - x)(\beta + x)$. This parabola has maximum value $y_{max} = (\frac{1+\beta}{2})^2$ at $x_{max} = (1 - \beta)/2$. The y-nullclines are the axis $y = 0$ and the line $x = \delta\beta/(1 - \delta)$. This line could be either to the left or right of the maximum of the parabola. If it is to the right, it may or may not intersect the parabola, depending on whether it is to the left or right of $x = 1$. One possible configuration of nullclines is shown in Figure 2.1.

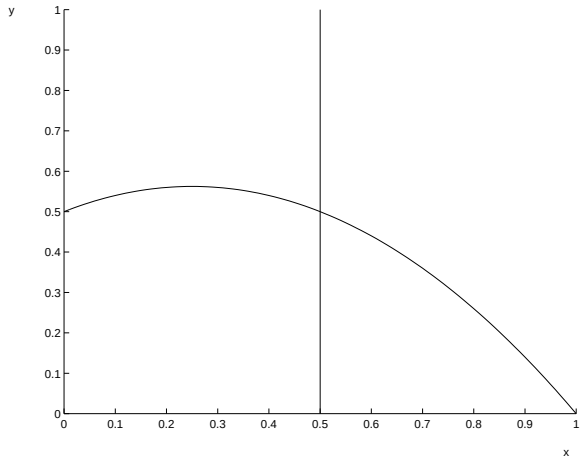

Figure 2.1: Possible intersection of the nullclines

The equilibria occur where the nullclines intersect, since at those points both derivatives are zero. If the y-nullcline line is to the right of $x = 1$, then there are two equilibria, $T = (0, 0)$ and $X = (1, 0)$. Otherwise there are three, T, X and

$$XY = \left(\frac{\delta\beta}{1 - \delta}, \frac{\beta - \beta\delta - \beta^2\delta}{(1 - \delta)^2} \right).$$

At T, both species die out. At X, the prey reach their carrying capacity and the predators die out. This happens if the death rate of the predator is too big (or if there are no predators to begin with). At XY the species coexist.

To determine the stability of each of these equilibria, we linearize equation (2.1) and determine the eigenvalues of the Jacobian at each equilibrium. If we do this, we will discover that T is always a saddle. It is only reached if we start off with no prey. X is a stable equilibrium if $\delta > 1/(\beta + 1)$. This corresponds to the y-nullcline line being to the right of $x = 1$ so that there are only two equilibria. In this case, the death rate of the predators is so high that their population cannot be sustained, even if the prey are at their carrying capacity. X is a saddle if $\delta < 1/(\beta + 1)$, and in that case, an orbit only reaches X if there are no predators to begin with. The equilibrium XY can be a stable or unstable spiral. It is stable if $\beta > \frac{1-\delta}{1+\delta}$. This corresponds to the y-nullcline line being to the right of the maximum of the parabola (but still intersecting the parabola). In this case, if we start with a positive amount of predator and prey then the orbit will approach this equilibrium. If instead $\beta < \frac{1-\delta}{1+\delta}$, then the y-nullcline line lies between $x = 0$ and $x = x_{max}$ and XY is an unstable spiral. As the y-nullcline crosses the line $x = x_{max}$, there is a Hopf bifurcation, and so a small periodic orbit appears, encircling the equilibrium XY. From the Hopf bifurcation theorem alone, we don't know if this periodic orbit persists after the y-nullcline line passes to the left of $x = x_{max}$. However, we can apply Kolmogorov's Theorem, which is stated in the appendix, to verify that this orbit does indeed persist. In the next section, we use singular perturbation analysis to better understand what this orbit looks like.

2.3 The Singular Orbit

In this section, we do further analysis to understand the dynamics for the case when $\beta < (1 - \delta)/(1 + \delta)$; that is, the y-nullcline line is to the left of x_{max}.

When the parameter ζ is very small, the populations develop on very different time scales. The prey population will quickly reach a place where $\dot{x} = 0$ before the predator population has had a chance to change very much. In this case, the dynamics of the prey are closely modelled by the *fast subsystem* which we obtain by rescaling time so that $\bar{t} = t/\zeta$ and then setting $\zeta = 0$.

$$\begin{aligned} \frac{dx}{d\bar{t}} &= xf(x, y) \\ \frac{dy}{d\bar{t}} &= 0 \end{aligned}$$

Orbits of the fast subsystem move only in the x-direction and tend towards the x-nullclines. In Figure 2.2 we show different orbits for several different initial conditions. Notice that solutions always tend towards either the right side of the parabola or the

nullcline $x = 0$. We say that the right side of the parabola is the *stable branch* of that nullcline. Let y^* denote the y-value where the two x-nullclines intersect and let y_0 denote the y-value of the initial condition. Notice that if $y^* < y_0 < y_{max}$, then there are three equilibria for the x-equation, two stable and one unstable. If we ignored the fact that we are only interested in positive values of x, then as y passes below y^*, the unstable equilibrium would switch to the negative side of $x = 0$ and would become stable, while $x = 0$ itself switches from stable to unstable. When two nearby equilibria switch stability, we call this a *transcritical bifurcation*. We rename y^*, y_{trc}.

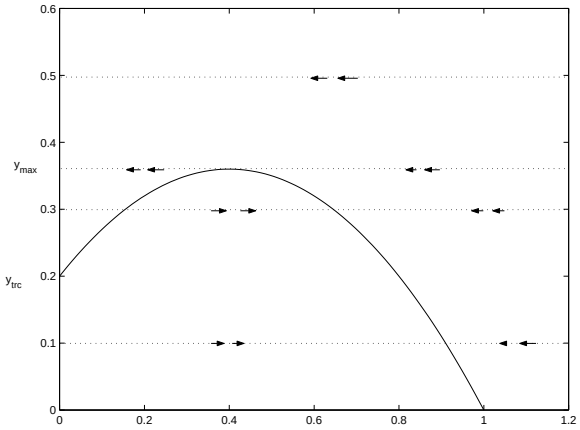

Figure 2.2: Orbits of the fast subsystem

Once the prey population has reached a nullcline, dx/dt becomes zero and now dy/dt dominates. If we let $\zeta = 0$ in equation (2.1) we get the slow subsystem.

$$\begin{aligned} 0 &= xf(x,y) \\ \tfrac{dy}{dt} &= yg(x) \end{aligned}$$

Orbits of the slow subsystem lie on the x-nullclines. If we start to the right of the y-nullcline line, we'll have $dy/dt > 0$ and y will increase. So the orbit goes up to the top of the parabola. At the top, the orbit is undefined. If we start on the parabola, but to the left of the y-nullcline, the orbit goes towards $y = y_{trc}$. If we start on $x = 0$, the orbit goes to $y = 0$. Movement of the slow orbits along the x-nullclines is indicated by arrows in Figure 2.3.

A singular orbit is constructed by "gluing together" fast and slow orbits. Suppose an initial condition begins off the parabola with $y_{trc} < y_0 < y_{max}$ and $x_0 > x_{max}$. Then

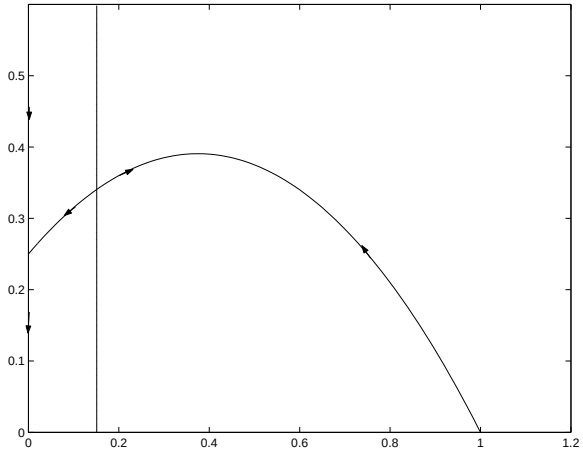

Figure 2.3: The slow flow when $\beta < \frac{1-\delta}{1+\delta}$

there is a fast orbit connecting the initial condition to the stable branch of the parabola. This fast orbit will be the first leg of the singular orbit. Once we get to the parabola, there is a slow orbit taking us to the top of the parabola. This is the second leg of the singular orbit. At the top of the parabola, there is a fast orbit connecting (x_{max}, y_{max}) to the nullcline $x = 0$. This is the third branch of the singular orbit. Once on $x = 0$, there is a slow orbit going downwards. At some point below $y = y_{trc}$, the singular orbit will follow a fast orbit back to the stable branch of the parabola (this is because $x = 0$ has now become unstable). This happens at a value of y, which we call y_{spk}, which satisfies the equation

$$0 = \int_{y_{spk}}^{y_{max}} \frac{f(0,y)}{yg(0,y)}\, dy$$

which upon integrating yields

$$\ln y_{spk} - \beta y_{spk} = \ln y_{max} - \beta y_{max}.$$

The last leg of the singular orbit follows a slow orbit up the parabola until it meets up with the second leg. Hence we have a singular periodic orbit (see Figure 2.4). It has been proved that if there is a singular periodic orbit then for small ζ there is a periodic orbit near the singular orbit (see [4]). In fact, numerical experiments show that this periodic orbit persists for fairly large values of ζ (see Figure 2.5).

One interesting thing to note is that along the periodic orbit the x-population gets dangerously low, while the y-population remains above y_{spk}. If anything perturbed the

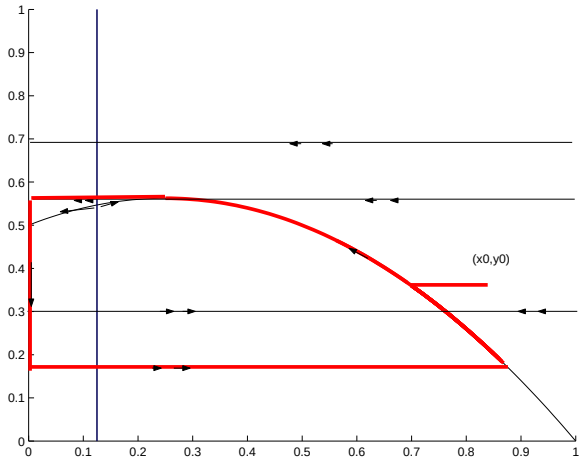

Figure 2.4: Singular periodic orbit for $\beta < \frac{1-\delta}{1+\delta}$

system while the x-population was small, they might all die out. Subsequently the y's would die out, too. Another interesting thing to notice is that when there is a periodic orbit the average y population is smaller than the y-population in the equilibrium point case. This is perhaps counterintuitive as one way to move the y-nullcline over is to decrease β which has the effect of increasing the efficiency of the predator. This is known as Rosenzwieg's Enrichment Paradox (see [5]).

2.4 Summary

For this model, we can find out a lot about the long term behavior of the populations just by determining the equilibria and their stability. When $\beta > (1-\delta)/(1+\delta)$, all solutions go to an equilibrium. However, we need to employ a more sophisticated method of analysis when $\beta < (1-\delta)/(1+\delta)$. Using Kolmogorov's Theorem, we know that there is a periodic orbit encircling the unstable equilibrium point and using singular perturbation analysis, we can get a rough idea of what this orbit looks like and we can understand some very important qualitative effects.

These same ideas will be used to analyze our food webs, but the pictures will become more complicated as another dimension is added.

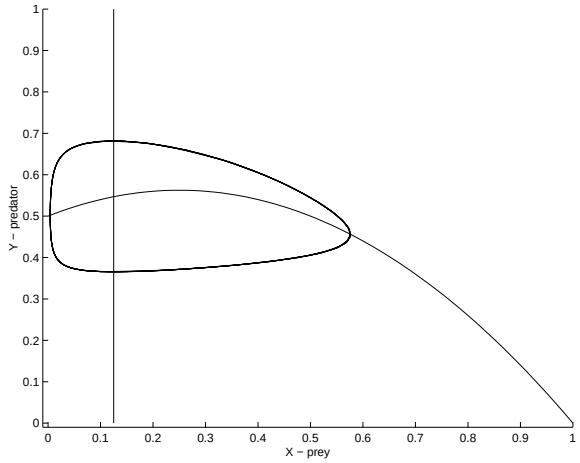

Figure 2.5: Periodic orbit for $\beta = 0.5$, $\delta = 0.2$, $\zeta = 0.1$

3 Simultaneously Available Prey

3.1 The Model

Now suppose that we have two prey available and that the predator makes no distinction between them, except that one is easier to catch. We can imagine repeating Holling's experiment, only now with two different size discs– the larger disc representing the easier prey. Following Holling's argument, we derive expressions for the amount of prey caught per predator, for each prey type. Let X and Y be the populations of the two different prey and Z be the population of the predator. Let X_c be the amount of prey-X caught per predator and Y_c be the amount of prey-Y caught per predator. Suppose that T is the total search time available to the predator. Let a_x and a_y be the instantaneous rates of discovery of X and Y respectively (the easier prey will have larger discovery rate). The rates a_x and a_y have units of $1/t$ per Z. Let H_x and H_y be the handling time for each prey. We can now give expressions for X_c and Y_c.

$$\begin{aligned} X_c &= a_x X(T - H_x X_c - H_y Y_c) \\ Y_c &= a_y Y(T - H_x X_c - H_y Y_c) \end{aligned}$$

The term $T - H_x X_c - H_y Y_c$ is the total time remaining for searching. If we solve the first equation for X_c and the second for Y_c, we get

$$\begin{aligned} X_c &= \frac{a_x X(T - H_y Y_c)}{1 + a_x X H_x} \\ Y_c &= \frac{a_y Y(T - H_x X_c)}{1 + a_y Y H_y} \end{aligned}$$

and then solving this system gives us

$$\begin{aligned} X_c &= \tfrac{a_x XT}{1+a_x H_x X+a_y H_y Y} \\ Y_c &= \tfrac{a_y YT}{1+a_x H_x X+a_y H_y Y}. \end{aligned}$$

Now we introduce some more parameters to simplify these expressions. Let $s = H_y/H_x$, $H = 1/a_x H_x$, $p = 1/H_x$ and $a = a_y/a_x$. Then we get

$$\begin{aligned} \tfrac{X_c}{T} &= \tfrac{pX}{H+X+asY} \\ \tfrac{Y_c}{T} &= \tfrac{apY}{H+X+asY}. \end{aligned}$$

If d is the death rate of the prey and b_x, b_y are the birth-to-consumption ratios of the prey, then we have the following model for the food web.

$$\begin{aligned} \tfrac{dX}{d\bar{t}} &= r_x X\left(1-\tfrac{X}{K_x}\right) - \tfrac{pX}{H+X+asY}Z \\ \tfrac{dY}{d\bar{t}} &= r_y Y\left(1-\tfrac{Y}{K_y}\right) - \tfrac{apY}{H+X+asY}Z \\ \tfrac{dZ}{d\bar{t}} &= -dZ + b_x\tfrac{pX}{H+X+asY}Z \ + b_y\tfrac{apY}{H+X+asY}Z \end{aligned}$$

If we rescale as before, using $x = X/K_x$, $y = Y/K_y$, $z = Zp/r_x K_x$ and $t = r_y\bar{t}$, then we get the nondimensional equations

$$\begin{aligned} \zeta\dot{x} &= x\left(1-x-\tfrac{z}{\beta+x+\sigma y}\right) := xf(x,y,z) \\ \dot{y} &= y\left(1-y-\tfrac{\mu z}{\beta+x+\sigma y}\right) := yg(x,y,z) \\ \dot{z} &= \epsilon z\left(\tfrac{x+\rho y}{\beta+x+\sigma y}-\delta\right) := \epsilon z h(x,y) \end{aligned} \tag{3.1}$$

where $\beta = H/K_x$, $\delta = d/b_x p$, $\epsilon = b_x/r_y$, $\mu = r_x a/r_y$, $\rho = b_y/b_x$, $\sigma = asK_x/K_y$ and $\zeta = r_y/r_x$. Writing the system in this form suggests that we might consider it as a singularly perturbed system if $0 < \zeta \ll 1$ and $0 < \epsilon \ll 1$. We will assume this in our analysis, though it will not be applicable in all cases.

3.2 Nullclines and Equilibria

In order to analyze (3.1), we determine the nullcline surfaces given by the equations $xf(x,y,z) = 0$, $yg(x,y,z) = 0$ and $zh(x,y,z) = 0$. First we determine the x-nullclines. The x-nullclines are the plane $x = 0$ and the surface $f(x,y,z) = 0$ which is more conveniently written $z = p(x,y) := (1-x)(\beta+x+\sigma y)$. This surface is parabolic with maximum value $z_{max} = (1+\beta+\sigma y)^2/4$ which occurs along the line $x_{max} = (1-\beta-\sigma y)/2$. The plane and the surface intersect in the transcritical line $z_{trc} = \beta + \sigma y$. See Figure 3.1.

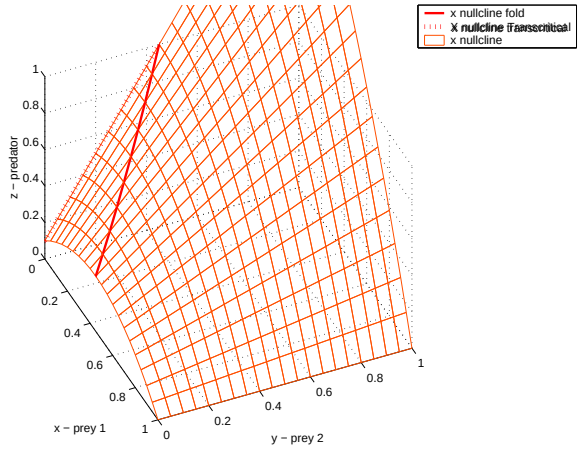

Figure 3.1: The x-nullcline surface showing the ridge line and the transcritical line

The y-nullclines are given by the plane $y = 0$ and the surface $z = q(x, y) := \frac{1}{\mu}(1 - y)(\beta + x + \sigma y)$. This surface is also parabolic with maximum value $z = \sigma(y-1)^2/\mu$ which occurs along the line $x = \sigma - \beta - 2\sigma y$. See Figure 3.2. The surface and the plane intersect in a line of transcritical points.

The z-nullclines are given by two planes $z = 0$ and $y = x\frac{\delta - 1}{\rho - \delta\sigma} + \frac{\delta\beta}{\rho - \delta\sigma}$.

The equilibria occur wherever an x-, y- and z-nullcline all intersect, since then all three derivatives are zero. If we solve for all of these intersections in the first quadrant, we come up with seven equilibria: $T = (0, 0, 0)$, $X = (1, 0, 0)$, $Y = (0, 1, 0)$, $XY = (1, 1, 0)$, and

$$\begin{aligned} XZ &= \left(\tfrac{\delta\beta}{1-\delta}, 0, (1 - \tfrac{\delta\beta}{1-\delta})(\beta + \tfrac{\delta\beta}{1-\delta})\right), \\ YZ &= \left(0, \tfrac{\delta\beta}{\sigma(1-\delta)}, \tfrac{1}{\mu}(1 - \tfrac{\delta\beta}{\sigma(1-\delta)})(\beta + \tfrac{\delta\beta}{1-\delta})\right), \\ XYZ &= (A, B, C) \end{aligned}$$

where $A = (-\mu\rho + \delta\sigma\mu + \rho - \delta\sigma - \delta\beta)/c$, $B = -(\delta\beta\mu + \delta\mu - \delta - \mu + 1)/c$ and $C = (\sigma\mu - \sigma - \beta - \mu\beta\rho - \mu\rho + \rho)(-1 + \delta - \rho + \delta\sigma + \delta\beta)/c^2$ and where $c = (-\mu\rho + \delta\sigma\mu - 1 + \delta)$. T is the trivial equilibrium where all populations are zero. X and Y are equilibria where only one prey survives (at its carrying capacity) and the predator dies out. At XY, both prey survive at their carrying capacities, but Z dies out. At XZ and YZ one prey survives and the predator survives. At XYZ all species co-exist.

In order to determine the stability of these equilibria, we can linearize (3.1) and determine the eigenvalues of the Jacobian matrix at each equilibria. If we do this, we discover

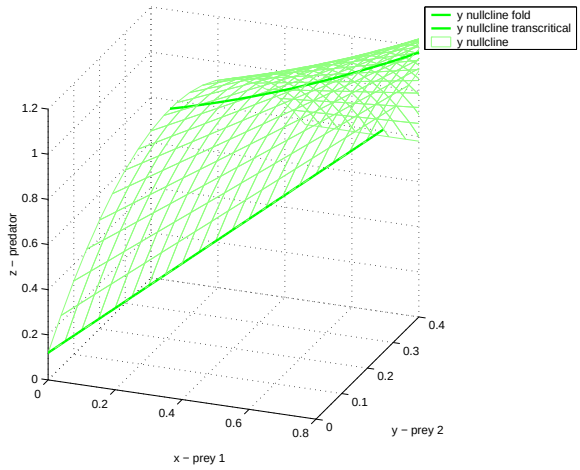

Figure 3.2: The y-nullcline surface showing the ridge line and the transcritical line

that T, X and Y are saddles. Only solutions which start on the axes will converge to one of these equilibria. XY is a stable equilibrium if $\delta < (1+\rho)/(1+\beta+\sigma)$ and a saddle otherwise. This condition on the parameters corresponds to the death rate of the predators being too high for their population to be sustained by the prey, even if the prey are at their carrying capacity. At the other three equilibria, XZ, YZ, and XYZ, the Jacobian is too complicated to analyze analytically. However, numerical experiments show that both XZ and YZ can be stable or unstable with periodic orbits around them. The periodic orbits lie on the $y = 0$ and $x = 0$ planes respectively. The equilibrium XYZ is sometimes stable and sometimes unstable. The stability of this point will be discussed further after we better understand the singular orbits.

3.3 Singular Orbits

If $0 < \zeta \ll 1$ and $0 < \epsilon \ll 1$, we have three time scales, each associated with the growth rate of a different species. If, as in the predator-prey case, we write down a model corresponding to each time scale, then we can construct a singular orbit by gluing together orbits from each of the three models. It can be proven that if there is a singular periodic orbit then for small ζ and ϵ there is also a periodic orbit and it lies near the singular orbit. These orbits may sometimes persist for even larger values of ϵ and ζ.

If ζ is small then $\dot{x} = \frac{1}{\zeta} x f(x,y,z)$ is large provided xf is not near zero and so the x-population changes very quickly. On this time scale the y- and z- populations are virtually constant. In fact, if we rescale time so that $\tau = t/\zeta$, then setting $\zeta = 0$ gives us the *fast*

subsystem:

$$\begin{aligned}\dot{x} &= x(1 - x - \tfrac{z}{\beta+x+\sigma y})\\ \dot{y} &= 0\\ \dot{z} &= 0.\end{aligned}$$

Orbits of the fast subsystem move only in the x-direction. They move towards an x-nullcline, where $\dot{x} = 0$. The destination of a fast orbit depends on the z-value of its initial condition, z_0. If $z_0 > z_{max}$, the orbit will go to the plane $x = 0$. If $z_0 < z_{trc}$, the orbit will go to to the so-called *stable branch* of the parabola $z = p(x, y)$ (that is, the part furthest from the $x = 0$ plane). If $z_{trc} < z_0 < z_{max}$, the orbit will go to $x = 0$ if the initial condition is between the plane $x = 0$ and the parabola, and to the stable branch of the parabola otherwise. Orbits of the fast subsystem are shown in Fig 3.3.

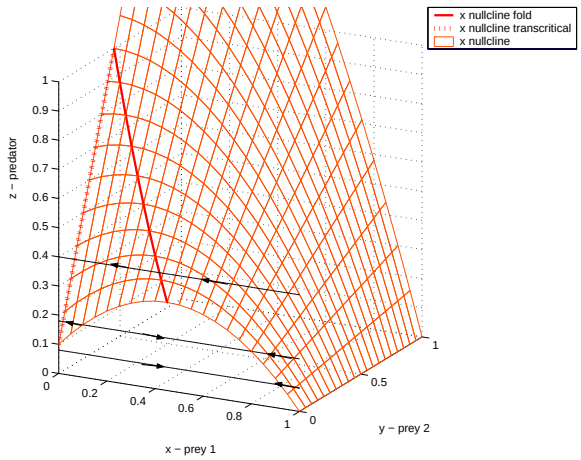

Figure 3.3: Orbits of the fast subsystem

If we let $\zeta = \epsilon = 0$, then we have the *intermediate subsystem* which develops on the time scale of the population y.

$$\begin{aligned}0 &= x\left(1 - x - \tfrac{z}{\beta+x+\sigma y}\right)\\ \dot{y} &= y\left(1 - y - \tfrac{\mu z}{\beta+x+\sigma y}\right)\\ \dot{z} &= 0.\end{aligned}$$

Orbits of this system must lie on one of the x-nullclines. Their movement along the x-nullcline is governed by the position of the orbit relative to the y-nullclines. So the form of the intersection of the x- and y-nullcline is important to this part of the analysis.

The nontrivial x- and y-nullclines intersect in a curve γ. Several possibilities are shown in Figure 3.4. Above γ we have $\dot{y} < 0$, so orbits move in the direction of decreasing y and below γ we have $\dot{y} > 0$, so orbits move in the direction of increasing y. If we start on the surface $z = p(x, y)$, then orbits will go towards γ, with constant z-value. If we start on the surface $x = 0$, then orbits will go to $y = 0$ (i.e. the z-axis), with constant z-value.

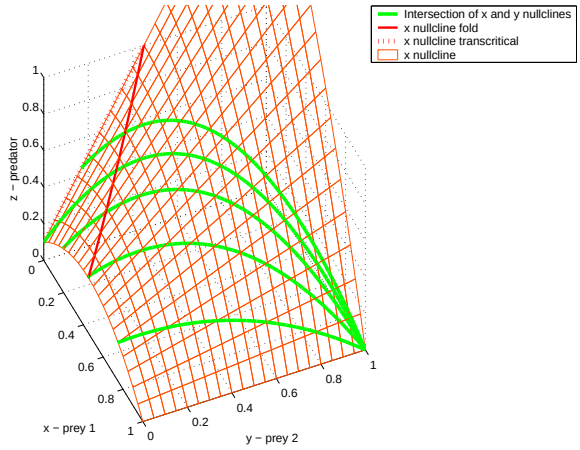

Figure 3.4: Possible intersections of the x- and y-nullclines

The slowest time scale is that of the z-population. If we rescale time so that $\tau = t\epsilon$ and then set $\epsilon = 0$, we get

$$\begin{aligned} 0 &= x\left(1 - x - \tfrac{z}{\beta+x+\sigma y}\right) \\ 0 &= y\left(1 - y - \tfrac{\mu z}{\beta+x+\sigma y}\right) \\ \dot{z} &= z\left(\tfrac{x+\rho y}{\beta+x+\sigma y} - \delta\right) \end{aligned}$$

This is the *slow subsystem*. Orbits of the slow subsystem must always lie on both the x- and y-nullclines. That is, orbits must always be on either γ or the z-axis. Orbits move along these curves in the direction of increasing z if they begin below the plane $y = x\frac{\delta-1}{p-\delta\sigma} + \frac{\delta\beta}{p-\delta\sigma}$, and in the direction of decreasing z if they begin above.

The construction of singular orbits for this model is much more complicated than that of the predator-prey system because several different configurations of the nullclines are possible, and each configuration leads to a different behavior. Let's first think about how the location of the z-nullcline affects the behavior of the system. Remember that the equilibrium XYZ lies at the intersection of the three nontrivial nullclines. If the z-nullcline plane is not too steep then this intersection will occur on the stable branch of the

nontrivial x-nullcline. Suppose we start with an initial condition for which the fast orbit goes to the stable branch. This fast orbit will be the first leg of our singular orbit. The remainder of the singular orbit will lie on the stable branch and will go towards XYZ. In fact, numerical experiments suggest that, regardless of the size of ζ and ϵ, if XYZ lies on the stable branch, then all solutions will go to XYZ. It is possible to give conditions on the parameters to ensure that XYZ lies on the stable branch. It can be shown that when $\delta = \delta^*$ where

$$\delta^* = -\frac{\beta - 2\sigma\mu + \mu\rho + \mu\beta\rho - \sigma\mu\rho - 2\rho + \sigma - 1}{1 + \beta\sigma\mu + \sigma^2\mu + \sigma\mu + \sigma + \beta},$$

XYZ lies on the ridge of the surface $z = p(x, y)$. If $\delta^* < \delta < (1 + \rho)/(1 + \beta + \sigma)$ then XYZ will lie on the stable branch. If $\delta < \delta^*$ then XYZ will lie on the unstable branch. In this case we have a singular periodic orbit. We discuss the nature of this orbit next.

When $\mu = 2/(1 + \beta)$, γ intersects the $y = 0$ plane at the ridge of the x-nullcline. If $\mu > 2/(1 + \beta)$, then γ will not intersect the ridge of the x-nullcline at all (see Figure 3.4) and if $\mu < 2/(1 + \beta)$ then γ will intersect the ridge at some point $y > 0$. Let's discuss this latter case first. In this case, a singular orbit beginning on the stable part of the x-nullcline will first approach γ and then travel along γ. The direction in which it travels along γ depends on the sign of $\dot{z}$, but in this case the stable branch lies below the z-nullcline plane and so $\dot{z} > 0$. Hence the singular obit travels up γ to the ridge of the parabolic surface $z = p(x, y)$. At the ridge, the singular orbit will follow a leg of the fast flow to the nullcline $x = 0$. Then it will follow a leg of the intermediate flow to the $y = 0$ nullcline, so that now it lies on the z-axis. Then it will follow a slow orbit, along the axis, in the direction of decreasing z. At some point, the singular orbit will return to the stable part of the parabola, as the plane $x = 0$ becomes unstable. This can happen either by first following a fast leg (in the x-direction) and then an intermediate leg (in the y-direction) or by first following an intermediate leg and then a fast leg. See Figures 3.5 and 3.6 for an orbit of each type. In each case, the value of z at which the singular orbit switches to another leg is determined by an integral formula. This is just like determining y_{spk} in the predator-prey case. Let z_{max} be the value of z when the singular orbit first arrived on the $x = 0$ nullcline (this will be the value of z at which γ intersects the fold line). If the singular orbit switches to a fast leg, then this happens at the value z_1 determined by

$$0 = \int_{z_1}^{z_{max}} \frac{f(0, 0, z)}{zh(0, 0, z)}\, dz$$

which upon integrating becomes

$$z_{max} - \beta \ln z_{max} = z_1 - \beta \ln z_1.$$

If the singular orbit switches to an intermediate leg, this happens at the value z_2 determined by

$$0 = \int_{z_2}^{z_{max}} \frac{g(0,0,z)}{zh(0,0,z)}\, dz$$

which upon integrating becomes

$$\mu z_{max} - \beta \ln z_{max} = \mu z_2 - \beta \ln z_2.$$

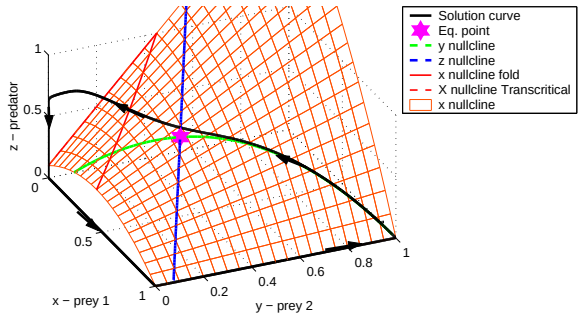

Figure 3.5: A singular orbit which returns via a fast leg

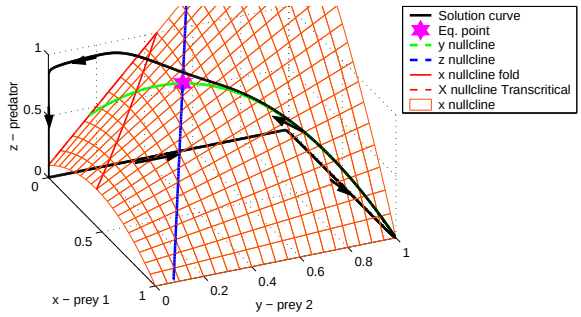

Figure 3.6: A singular orbit which returns via an intermediate leg

Whether the singular orbit first switches to a fast leg or first switches to an intermediate leg is determined by whether z_1 or z_2 is bigger. If $z_2 > z_1$ then a singular orbit coming down the z-axis will first switch to an intermediate flow and then a fast flow. If $z_1 > z_2$ then it will first switch to a fast flow and then an intermediate flow. It is not hard to show that $z_2 > z_1$ if and only if $\mu < 1$.

When the singular orbit returns to the stable branch of the parabola, it switches to an intermediate leg which goes to the curve γ and then it switches to the final slow leg which moves up γ to join up with the second leg. Thus there is a singular periodic orbit which persists at least for small ζ and ϵ. In fact, numerical experiments suggest that this orbit persists for fairly large values of ζ and ϵ. Some of these orbits are shown in Figures 3.7 and 3.8.

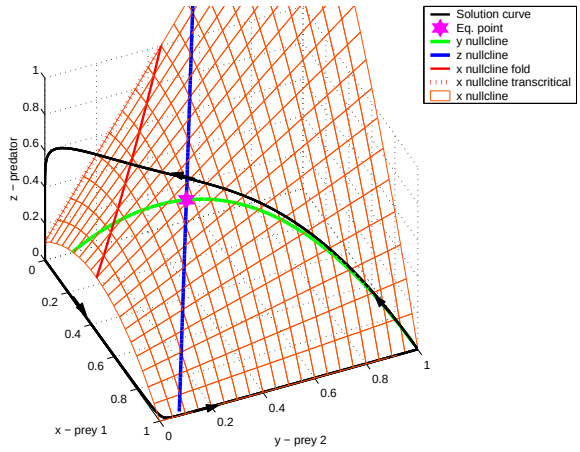

Figure 3.7: A nonsingular orbit which returns via a fast leg

So far, we have avoided the case when $\mu = 1$. Then $z_1 = z_2$. Numerical experiments for nonzero ζ and ϵ indicate that in this case something a little bit different happens. The orbit returns along a curve which lies just above $z = 0$. The shape of this curve is heavily influenced by the value of σ. Figure 3.9 shows one case with $\zeta = 0.7$.

Now we consider the case when $\mu > 2/(1 + \beta)$. In this case the curve γ does not intersect the ridge of the parabolic surface $z = p(x, y)$. This means that once the singular orbit is on the stable branch, there is no mechanism for it to jump over to $x = 0$ and in fact it will remain on the stable branch for all future time. The analysis of the singular orbit on the stable branch is now a two-dimensional problem and much like the analysis we did in the predator-prey model. If XYZ lies on the stable branch of γ, then orbits will approach it. If XYZ lies on the unstable branch of γ, then the singular orbit will be periodic. Figure 3.10 shows such an orbit. In that case there will be a periodic orbit (near the singular orbit) at least for small values of ζ and ϵ.

All of this analysis, along with further numerical experiments, indicates that all solutions of the full system 3.1 approach either an equilibrium or a periodic orbit.

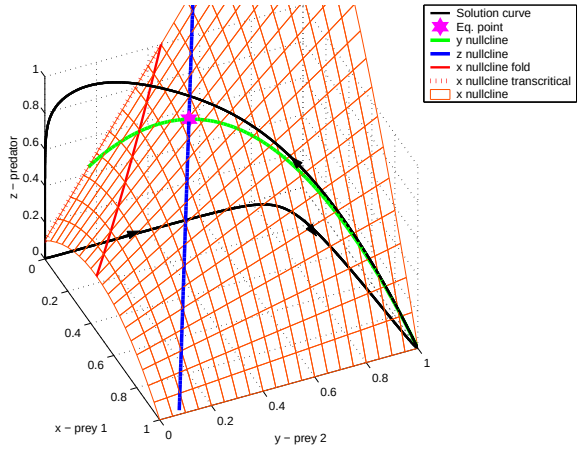

Figure 3.8: A nonsingular orbit which returns via an intermediate leg

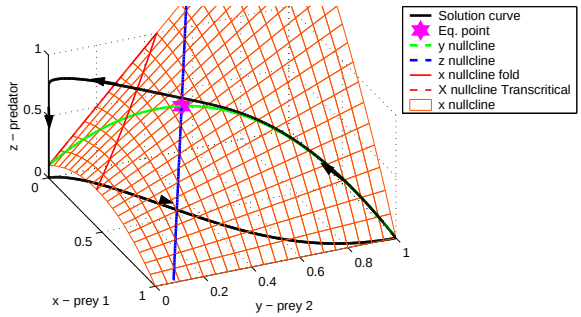

Figure 3.9: A periodic orbit when $\mu = 1$

3.4 Summary

What we have learned about the behavior of the orbits can be summarized as follows

- If $\delta^* < \delta < (1+\rho)/(1+\beta+\sigma)$ then XYZ lies on the stable branch of $z = p(x, y)$ and orbits tend towards XYZ.
- If $0 < \delta < \delta^*$, then XYZ lies on the unstable branch and there exists a singular periodic orbit. The shape of this orbit depends on μ and β. We have three cases.
  - If $\mu > 2/(1+\beta)$ then the singular orbit lies entirely on the stable branch.
  - If $1 < \mu < 2/(1+\beta)$ then the singular orbit jumps between the stable branch and $x = 0$. When it jumps from $x = 0$ to the stable branch it first follows a

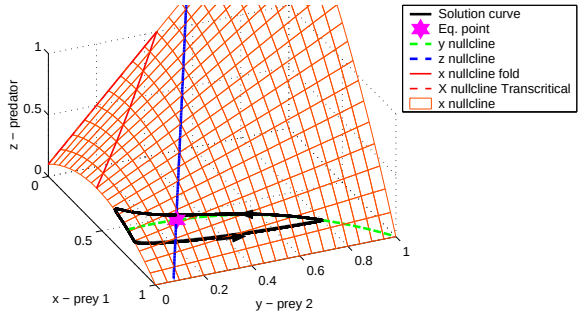

Figure 3.10: A singular orbit lying on the stable branch of the x-nullcline surface when $\mu > \frac{2}{1=\beta}$

fast leg and then an intermediate leg.

– If $\mu < 1$ then the singular orbit jumps between the stable branch and $x = 0$. When it jumps from $x = 0$ to the stable branch it first follows an intermediate leg and then a fast leg.

From the theory we know that for small values of ζ and ϵ the singular orbits persist. Numerical experiments show that this holds even for fairly large values of ζ and ϵ.

4 Disjointly Available Prey

4.1 The Model

Again we let X and Y be the prey and Z the predator. This time we assume that the two prey are not available at the same time. If T is the total amount of time the predator has available for searching, then suppose αT is the time the predator spends searching for prey X and $(1-\alpha)T$ is the time spent searching for predator Y. The parameter α is a fixed constant. This could be the case for example when one prey is nocturnal and the other is diurnal. If again we let X_c and Y_c be the amount of prey caught per predator, a_x and a_y the discovery rates for each prey and H_x and H_y the handling times, then

$$\begin{aligned} X_c &= a_x X(\alpha T - H_x X_c) \\ Y_c &= a_y Y((1-\alpha)T - H_y Y_c). \end{aligned}$$

If we solve each equation for X_c and Y_c, we get

$$\begin{aligned} \frac{X_c}{T} &= \frac{\alpha a_x X}{1+a_x H_x X} = \frac{p_x X}{q_x + X} \\ \frac{Y_c}{T} &= \frac{(1-\alpha) a_y Y}{1+a_y H_y Y} = \frac{p_y Y}{q_y + Y} \end{aligned}$$

where $p_x = \alpha/H_x$, $p_y = (1-\alpha)/H_y$ and $q_i = 1/a_i H_i$. Again assuming the prey grow logistically in the absence of predators and the predator dies exponentially in the absence of prey, we get the model

$$\begin{aligned}
\frac{dX}{d\bar{t}} &= r_x X(1 - \frac{X}{K_x}) - \frac{p_x X}{q_x + X} Z \\
\frac{dY}{d\bar{t}} &= r_y Y(1 - \frac{Y}{K_y}) - \frac{p_y Y}{q_y + Y} Z \\
\frac{dZ}{d\bar{t}} &= \frac{b_x p_x X}{q_1 + X} Z + \frac{b_y p_y Y}{q_2 + Y} Z - dZ
\end{aligned}$$

If we rescale as before now using the variables

$$\begin{aligned}
x &= X/K_x \\
y &= Y/K_y \\
z &= \frac{Z p_y}{r_y K_y} \\
t &= r_y \bar{t}
\end{aligned}$$

and parameters $\beta_i = q_i/K_i$, $\epsilon = b_y p_y / r_y$, $\delta = d/b_y p_y$, $\mu = r_y K_y / r_x K_x p_y$, $\sigma = b_x p_x / b_y p_y$, $\zeta = r_y / r_x$, then we get the nondimensionalized model

$$\begin{aligned}
\zeta \dot{x} &= x\left(1 - x - \frac{\mu z}{\beta_x + x}\right) := x f(x,z) \\
\dot{y} &= y\left(1 - y - \frac{z}{\beta_y + y}\right) := y g(y,z) \\
\dot{z} &= \epsilon x\left(\frac{\sigma x}{\beta_x + x} + \frac{y}{\beta_y + y} - \delta\right) := \epsilon z h(x,y)
\end{aligned} \tag{4.1}$$

Again, if $0 < \zeta \ll 1$ and $0 < \epsilon \ll 1$, the system is singularly perturbed, and so we can gain some understanding of the behavior of the system through singular perturbation analysis. First we determine the nullclines and equilibria.

4.2 Nullclines and Equilibria

In order to analyze (4.1), we determine the nullcline surfaces given by the equations $xf(x,z) = 0$, $yg(y,z) = 0$ and $zh(x,y) = 0$. The nullclines are shown in Figure 4.1. The x-nullclines are $x = 0$ and $z = \frac{1}{\mu}(1-x)(\beta_x + x)$. The nontrivial surface is parabolic with maximum $z_{max1} = (1+\beta_x)^2/4\mu$ at $x = (1-\beta_x)/2$. Notice that the maximum value is independent of x and y. This surface intersects $x = 0$ in the line $z = z_{trc1}$. The y-nullclines are $y = 0$ and $z = (\beta_y + y)(1-y)$. Again the nontrivial nullcline is parabolic with maximum value $z_{max2} = (1+\beta_y)^2/4$ at $y = (1-\beta_y)/2$ and the maximum value is independent of x and y. This surface intersects $y = 0$ in the line $z = z_{trc2}$. The z-nullclines are $z = 0$ and

$$x = \frac{((1-\delta)y - \delta\beta_y)\,\beta_x}{(\sigma + 1 - \delta)y + (\sigma - \delta)\beta_y}$$

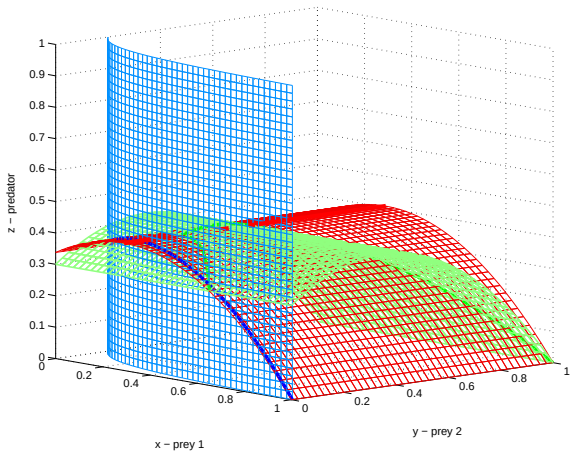

Figure 4.1: One possible nullcline configuration

The nontrivial nullcline is hyperbolic and its maximum is independent of y and z.

There are many different configurations of the three nullclines. We always have the trivial and semitrivial equilibria $T = (0, 0, 0)$, $XY = (1, 1, 0)$, $XZ = (\delta\beta/(\sigma - \delta), 0, (1 - x)(\beta_x + x)/\mu)$ and $YZ = (0, \beta_y\delta/(1 - \delta), (1 - y)(\beta_y + y))$. These have stability properties similar to those for the simultaneously available prey model. This case differs from the simultaneously available case though in that, depending on the relative positions of the nullclines, there could be one, two or three co-existence equilibria. The stability of these equilibria depend on the parameter values.

4.3 Singular Orbits

We obtain the fast subsystem by rescaling time according to the timescale of prey x. That is, we let $\bar{t} = t/\zeta$. Then, taking $\zeta = 0$, we have

$$\begin{aligned} \dot{x} &= x\left(1 - x - \tfrac{\mu}{\beta_x + x} z\right) \\ \dot{y} &= 0 \\ \dot{z} &= 0. \end{aligned}$$

The orbits for this system move only in the x-direction, with constant y and z. If the initial condition satisfies $z_0 > z_{max1}$, then the orbit goes to the $x = 0$ plane. If $z_{trc1} < z_0 < z_{max1}$, then the orbit goes to either $x = 0$ or the stable branch of the nontrivial nullcline. If $z < z_{trc}$, the orbit goes to the stable branch of the nontrivial nullcline.

We obtain the intermediate subsystem by letting $\epsilon = \zeta = 0$.

$$\begin{aligned} 0 &= x\left(1 - x - \tfrac{\mu}{\beta_x + x} z\right) \\ \dot{y} &= y\left(1 - y - \tfrac{1}{\beta_y + y} z\right) \\ \dot{z} &= 0 \end{aligned}$$

Orbits for the intermediate system lie on the x-nullcline and remain constant in z. Let γ_1 be the intersection of the stable branch of the x-nullcline with the y-nullcline. If $z_{max1} < z_{max2}$ then this will be in two pieces (see Figure 4.2). Let γ_2 be the intersection of the nontrivial y-nullcline with the trivial x-nullcine. If the initial condition lies on the stable branch of the nontrivial x-nullcline, then if $z_0 > z_{max2}$ then the orbit goes to the plane $y = 0$, if $z_{trc2} < z_0 < z_{max2}$, then the orbit goes to either $y = 0$ or the stable branch of γ_1, and if $z_0 < z_{trc2}$ then the orbit goes to the stable branch of γ_1 (we see this in Figure 4.3 for the case when $z_{max1} > z_{max2}$). If the initial condition lies on the trivial x-nullcline, then we can make a similar statement, only replacing γ_1 with γ_2 (see Figure 4.4).

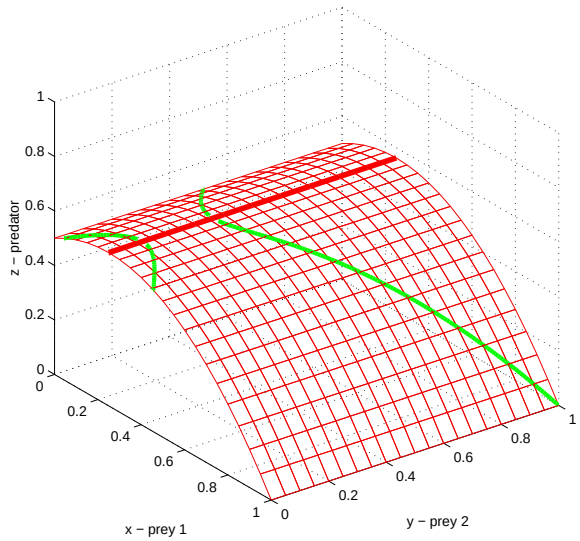

Figure 4.2: The intersection of the x- and y-nullclines when $z_{max2} > z_{max1}$

We obtain the slow subsystem by rescaling according the growth rate of z. So if $\bar{t} = t\epsilon$,

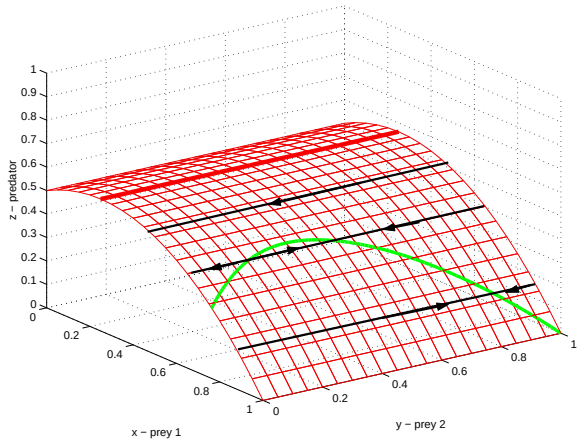

Figure 4.3: The intermediate flow on the stable branch when $z_{max1} > z_{max2}$

we get

$$\begin{aligned} 0 &= x\left(1 - x - \tfrac{\mu}{\beta_x + x} z\right) \\ 0 &= y\left(1 - y - \tfrac{1}{\beta_y + y} z\right) \\ \dot{z} &= x\left(\tfrac{\sigma x}{\beta_x + x} + \tfrac{y}{\beta_2 + y} - \delta\right) \end{aligned}$$

The orbits of this system are restricted to the curves γ_1, γ_2 and the intersection of the nontrivial x-nullcline with $y = 0$, which we will call γ_3. They move in the direction of increasing or decreasing z, depending on which side of the nontrivial z-nullcline they lie.

The singular orbits depend on the relative positions of the nullclines and there are a lot of possibilities.

If the nontrivial z-nullcline intersects the stable branch of γ_1, then there will be a stable co-existence equilibrium.

If $z_{max1} < z_{max2}$ (which happens when $\mu > (1 + 2\beta_x + \beta_x^2)/(1 + 2\beta_y\beta_y^2)$), and the z-nullcline intersects the unstable branches of γ_1 and γ_2, then there will be a singular periodic orbit on the $x = 0$ plane. Figure 4.5 shows the corresponding orbit for small ϵ and ζ. Other positions of the z-nullcline can lead to other behaviors when $z_{max1} < z_{max2}$. We can get a stable equilibrium on the $x = 0$ nullcline if the z-nullcline intersects the stable part of γ_2 (see Figure 4.6 for small ϵ and ζ). We can get a periodic orbit that oscillates between the two x-nullclines. We can even get a homoclinic orbit.

If instead $z_{max1} > z_{max2}$ and so γ_1 is one piece, we can get a periodic orbit lying on the stable branch of the x-nullcline. This periodic orbit will persist for small ζ and ϵ (see

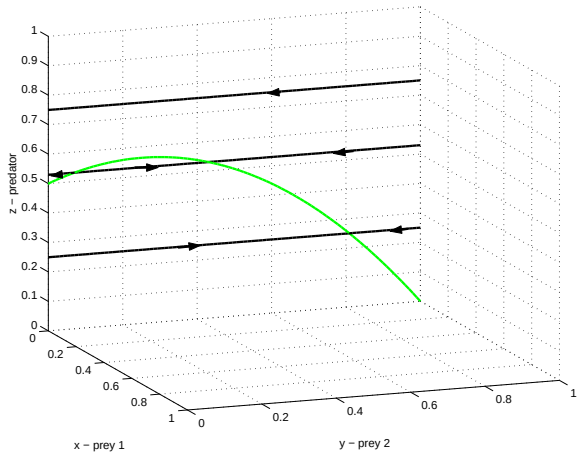

Figure 4.4: The intermediate flow on the trivial x-nullcline

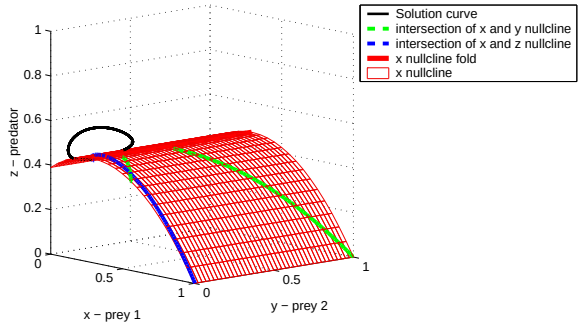

Figure 4.5: Periodic orbit on the $x = 0$ nullcline surface

Figure 4.7). Numerically, we discovered that if we relax ϵ (i.e. allow it to be a little bigger) this orbit may reach the top of the x-nullcline and so jump over to the $x = 0$ nullcline. This can lead to a complicated periodic orbit such as that shown in Figure 4.8. Relaxing ϵ a little bit more, we can even obtain chaotic singular orbits! We computed the Lyapunov exponents for the orbit shown in Figure 4.9 and obtain approximately .0049, .00003128, and -65. This means there is a small positive Lyapunov exponent, which though small is significant as time-scaling the model also scales the Lyapunov exponent. The exponent would be larger for the original unscaled system.

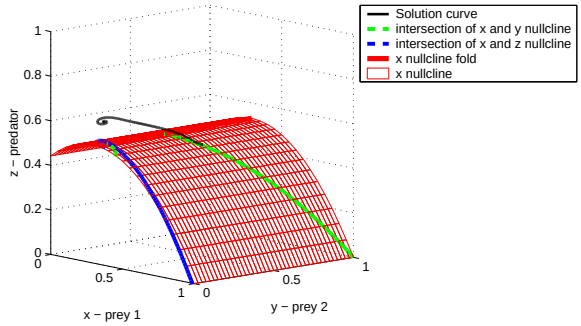

Figure 4.6: Stable equilibrium point on the $x = 0$ plane

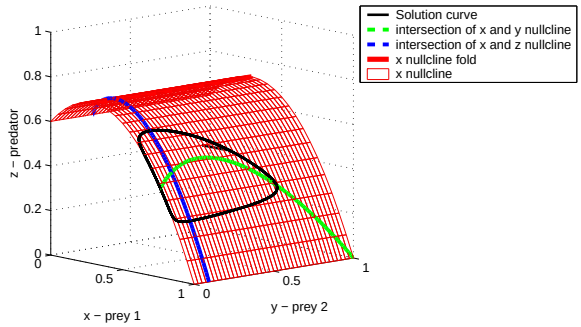

Figure 4.7: Periodic orbit on the stable $f = 0$ nullcline surface

5 Conclusions

In the case where the prey are simultaneously available, the dynamics are similar to those of the predator-prey problem. In fact, if we lump the two prey together and graph z versus $x + \sigma y$, we get a picture that is very similar to that of the predator-prey problem. This is shown in Figure 5.1 for two different sets of parameter values. Depending on the parameters, orbits always go to either an equilibrium or a periodic orbit.

In the case when the prey are available only one at a time, we can get more complicated dynamics. This is perhaps counterintuitive, but results from the more complicated nature of the nullclines. In this case, orbits can go to equilibria or simple periodic orbits as before, but we may also get more complicated periodic orbits and even chaotic orbits.

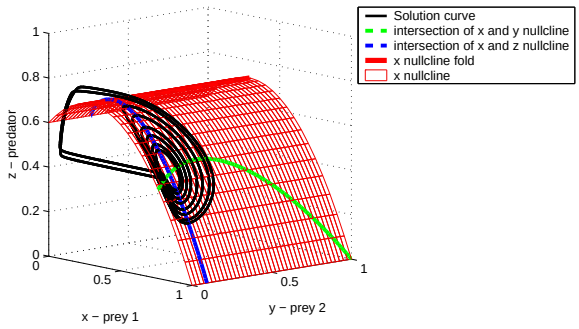

Figure 4.8: Cycle on the $f = 0$ nullcline with relaxed ϵ, showing complicated behavior

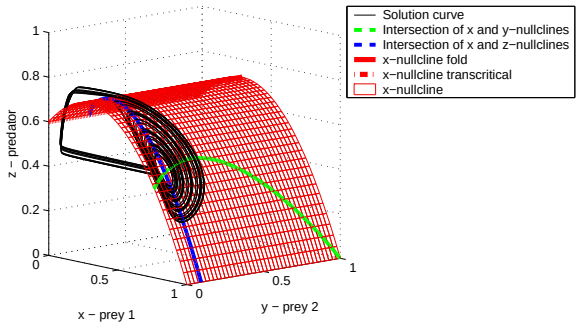

Figure 4.9: Chaos

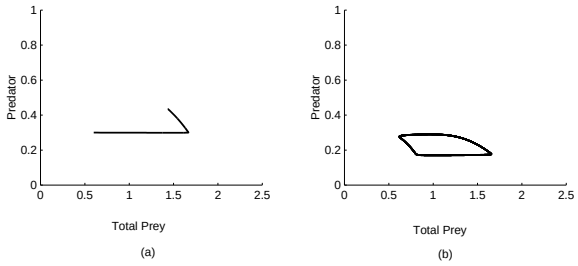

Figure 5.1: Plots of total prey against predator

6 Appendix

Theorem A1 (A.N. Kolmogorov, 1936) Consider a system of equations for $x, y \geq 0$.

$$\begin{aligned} \frac{dx}{dt} &= xf(x,y) \\ \frac{dy}{dt} &= yg(x,y) \end{aligned}$$

and assume the following conditions hold.

1. $f(0,0) > 0$
2. $\frac{\partial f}{\partial y} < 0$
3. $\frac{\partial g}{\partial y} \leq 0$
4. $x\frac{\partial f}{\partial x} + y\frac{\partial f}{\partial y} < 0$
5. $x\frac{\partial g}{\partial x} + y\frac{\partial g}{\partial y} > 0$
6. There exist constants $A > 0$, $B > 0$ and $C > 0$ such that $f(0,A) = f(B,0) = g(C,0) = 0$.

Then the system has either a stable equilibrium or a stable periodic orbit.

References

[1] C.S. Holling, Some Characteristics of Simple Types of Predation and Parasitism, *The Canadian Entomologist* **41** (1959) 385-398.

[2] I. Hanski, P. Turchin, E. Korpimaki and H. Heuttonen, Population Oscillations of Boreal ROdents: Regulation by Mustelid Predator Leads to Chaos, *Nature*, 364(1993), 232-235.

[3] L.A. Real, Ecological Determinants of Functional Response, *Ecology*, 60(1979), 481-485.

[4] S. Schechter, Persistent Unstable Equilibria and Closed Orbits of a Singularly Perturbed Equation, *J. Diff. Eq.*, 60(1985), 131-141.

[5] M.L. Rosezweig, Paradox of Enrichment: Destablization of Exploitation Ecosystems in Ecological Time, *Science*, 171(1971), 385-387.